Current Biology *16*, 660–667, April 4, 2006 ©2006 Elsevier Ltd All rights reserved DOI 10.1016/j.cub.2006.01.066

Report

Postmeiotic Sex Chromatin in the Male Germline of Mice

Satoshi H. Namekawa,[1] Peter J. Park,[2] Li-Feng Zhang,[1] James E. Shima,[3,5] John R. McCarrey,[4] Michael D. Griswold,[3] and Jeannie T. Lee[1,*]
[1] Howard Hughes Medical Institute
Department of Molecular Biology
Massachusetts General Hospital
Department of Genetics
Harvard Medical School
Boston, Massachusetts 02114
[2] Children's Hospital Informatics Program
Harvard-Partners Center for Genetics and Genomics
Boston, Massachusetts 02115
[3] Center for Reproductive Biology
School of Molecular Biosciences
Washington State University
Pullman, Washington 99164
[4] Department of Cellular and Structural Biology
University of Texas Health Sciences Center
at San Antonio
San Antonio, Texas 78249

Summary

In mammals, the X and Y chromosomes are subject to meiotic sex chromosome inactivation (MSCI) during prophase I in the male germline, but their status thereafter is currently unclear. An abundance of X-linked spermatogenesis genes has spawned the view that the X must be active [1–8]. On the other hand, the idea that the imprinted paternal X of the early embryo may be preinactivated by MSCI suggests that silencing may persist longer [9–12]. To clarify this issue, we establish a comprehensive X-expression profile during mouse spermatogenesis. Here, we discover that the X and Y occupy a novel compartment in the postmeiotic spermatid and adopt a non-RabI configuration. We demonstrate that this postmeiotic sex chromatin (PMSC) persists throughout spermiogenesis into mature sperm and exhibits epigenetic similarity to the XY body. In the spermatid, 87% of X-linked genes remain suppressed postmeiotically, while autosomes are largely active. We conclude that chromosome-wide X silencing continues from meiosis to the end of spermiogenesis, and we discuss implications for proposed mechanisms of imprinted X-inactivation.

Results

Postmeiotic Sex Chromatin: A Novel Nuclear Compartment

In mice, spermatogenesis requires 3 weeks and includes meiosis and spermiogenesis (Figure 1A) [13]. During meiosis, the XY spermatocyte undergoes two division rounds (meiosis I and II) to generate four haploid spermatids that bear either an X or a Y. During spermiogenesis (2 weeks), the spermatid is functionally transformed into mature spermatozoa. To examine the XY transcriptional status at each stage, we carried out Cot-1 RNA fluorescence in situ hybridization (FISH) on smears of seminiferous tubules (Figure 1). Cot-1 sequences are enriched for repetitive DNA and occur in the introns of nascent transcripts. Thus, hybridization of RNA to Cot-1 probes delineates domains of new transcription [10, 14]. After RNA FISH, we performed DNA FISH with X- or Y-painting probes to identify the sex chromosomes.

Types A and B spermatogonia are premeiotic cells bearing unsynapsed sex chromosomes and distinct pericentric heterochromatin (DAPI intense). In such cells, RNA/DNA FISH demonstrated pannuclear Cot-1 signals suggestive of genome-wide transcription (Figure 1B). While the X was clearly transcribed, the heterochromatic Y lay within a "Cot-1 hole." In the primary spermatocyte, the inactivated "XY body" becomes evident for the first time. At pachytene, the peripherally located XY body excluded Cot-1 hybridization in all cells examined (Figure 1C; n = 100), consistent with MSCI. The XY body also excluded the active form of RNA polymerase II (see Figure S1A in the Supplemental Data available with this article online).

To determine what happens after the XY body dissolved, we examined secondary spermatocytes, a transient cell type distinguishable from others by their reduction to one sex chromosome and their lack of a prominent chromocenter. RNA FISH showed that the X and Y continued to exclude Cot-1 hybridization and adopted a DAPI-intense appearance reminiscent of an XY body (Figures 1D and 1E). This indicated that, despite the dissolution of the XY body, the X remained undertranscribed. Furthermore, that transcriptional suppression continued into spermiogenesis (16 steps). Distinguished by their occurrence as "tetrads" of X- and Y-bearing nuclei with prominent chromocenters, steps 1–8 round spermatids demonstrated Cot-1 holes coincident with all X and Y domains (Figures 1F–1H; 100% of Xs with Cot-1 holes, n = 66; 100% of Ys with Cot-1 holes, n = 63), as well as coincident Pol-II holes (Figures S1B and S1C). Intriguingly, the X and Y were uniquely DAPI intense among all chromosomes and occupied a position alongside the chromocenter (Figures 1F–1H).

During the elongating spermatid stage (steps 9–11), we observed a progressive decrease in Cot-1 signals, consistent with the replacement of histones by protamines. In step 9 (Figures 1I and 1J), Cot-1 signals could be observed in 79% of nuclei (n = 56). Among spermatids with residual Cot-1 signals, the X and Y continued to exclude Cot-1 hybridization (Figures 1I and 1J; 100%, n = 44). By steps 10 (Figures 1K and 1L) and 11 (Figures 1M and 1N), general transcription appeared to cease, as shown by the pannuclear loss of Cot-1 signals.

*Correspondence: lee@molbio.mgh.harvard.edu
[5] Present address: Department of Biopharmaceutical Sciences, University of California at San Francisco, San Francisco, California 94243.

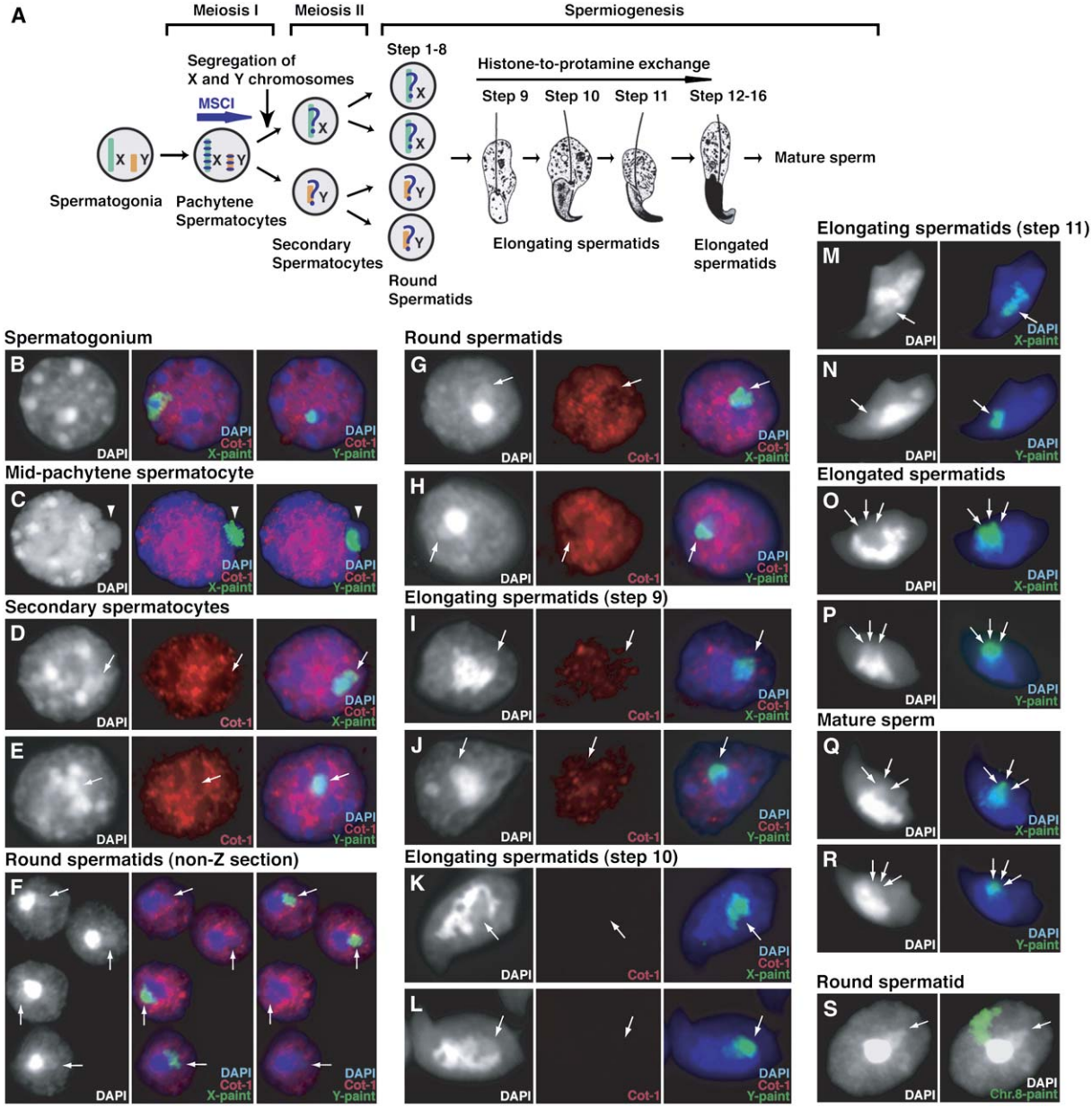

Figure 1. Discovery of Postmeiotic Sex Chromatin and Its Continuity to the End of Spermiogenesis

(A) Schematic of spermatogenesis. ?, unclear status of X and Y activity after MSCI. Spermiogenesis was staged according to the standard method [13]. The panel is partly adapted from Russell et al. [13]. Reprinted with permission from Cache River Science, an imprint of Quick Publishing, LC, 888-PUBLISH, fax 314-993-4485, email cacheriverpress@sbcglobal.net.

(B–R) For the cell types indicated on each panel, shown are Cot-1 RNA FISH (red signals), and/or chromosome-specific FISH of the X or Y (green signals).

(S) Radial arrangement of the autosome (Chr. 8) in RS. In contrast, the sex chromosomes adopt a compact, perichromocenter configuration. All images except (F) are single z-sections. Arrowhead, XY body. Arrows, PMSC.

Despite nuclear symmetry loss and chromocenter deformation, both X and Y were still discernible as DAPI-intense juxtachromocenter structures (Figures 1I–1N). Significantly, the XY body-like structure persisted in elongated spermatids (steps 12–16) and in mature spermatozoa (Figures 1O–1R). Therefore, contrary to current understanding [1–4, 6], the transcriptional suppression initiated by MSCI does not end with meiosis I, but rather continues into meiosis II and spermiogenesis long after the dissolution of the XY body.

We term this new structure "postmeiotic sex chromatin" (PMSC) and suggest that it may have been overlooked previously [5] because of sensitivity to experimental conditions. When subjected to hypotonic nuclear swelling, PMSC and its associated Cot-1 or pol-II holes are easily lost (Figure S2). In the course of our analysis, we also noted that both X- and Y-PMSC in the spermatid exhibited distinct chromosome configuration as compared to autosomes. Chromosome-specific painting revealed that, while autosomes were

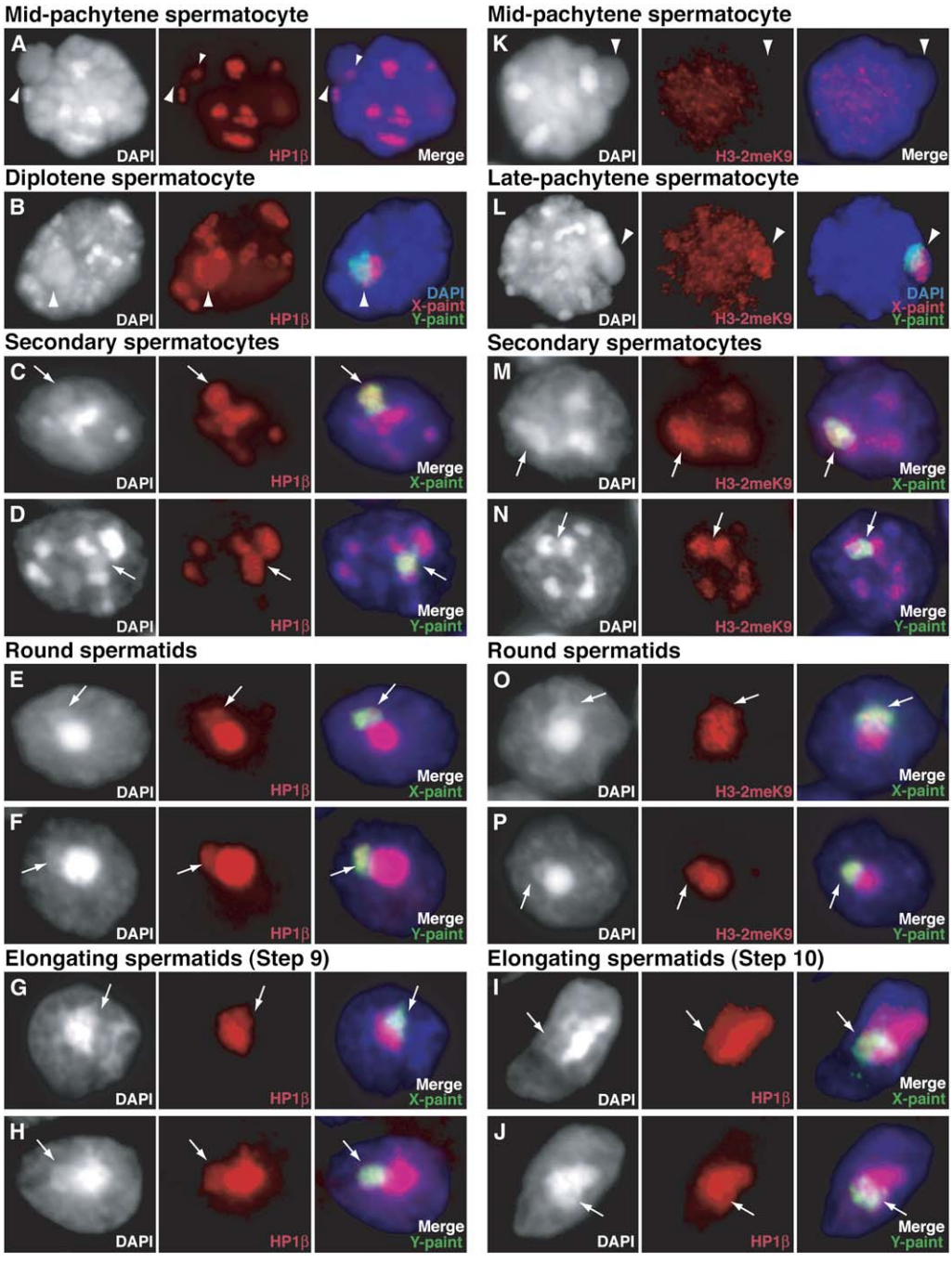

Figure 2. The XY Body and PMSC Are Similarly Marked by H3-2meK9 and HP1β

Immunofluorescence detecting H3-2meK9 or HP1β marks (red signals) in the cell types noted. All images are single z-sections. Arrowheads, XY body. Arrows, PMSC.

organized radially around the chromocenter in a Rabl configuration [15], the X and Y occupied a compact juxtachromocenter domain that did not extend to the nuclear periphery (Figure S1 and data not shown).

The Epigenetic Character of the XY Body and PMSC

To determine whether the chromatin is significantly remodelled during the XY body to PMSC transition, we followed the epigenetic profiles during spermatogenesis. Here, we found that HP1β localized first to the XY centromeres at midpachytene and spread through the XY body only during diplotene (Figures 2A and 2B) [16]. We further observed that HP1β also marked the X and Y in secondary spermatocytes (Figures 2C and 2D) and round spermatids (Figures 2E and 2F; 100% of X-PMSC, n = 112; 100% of Y-PMSC, n = 117). Indeed, HP1β could be detected on PMSC until the replacement of histones with protamines (Figures 2G–2J; 100% at steps 9–10, n = 69; 0% at step 11 and after). Similar results were obtained for HP1γ (data not shown).

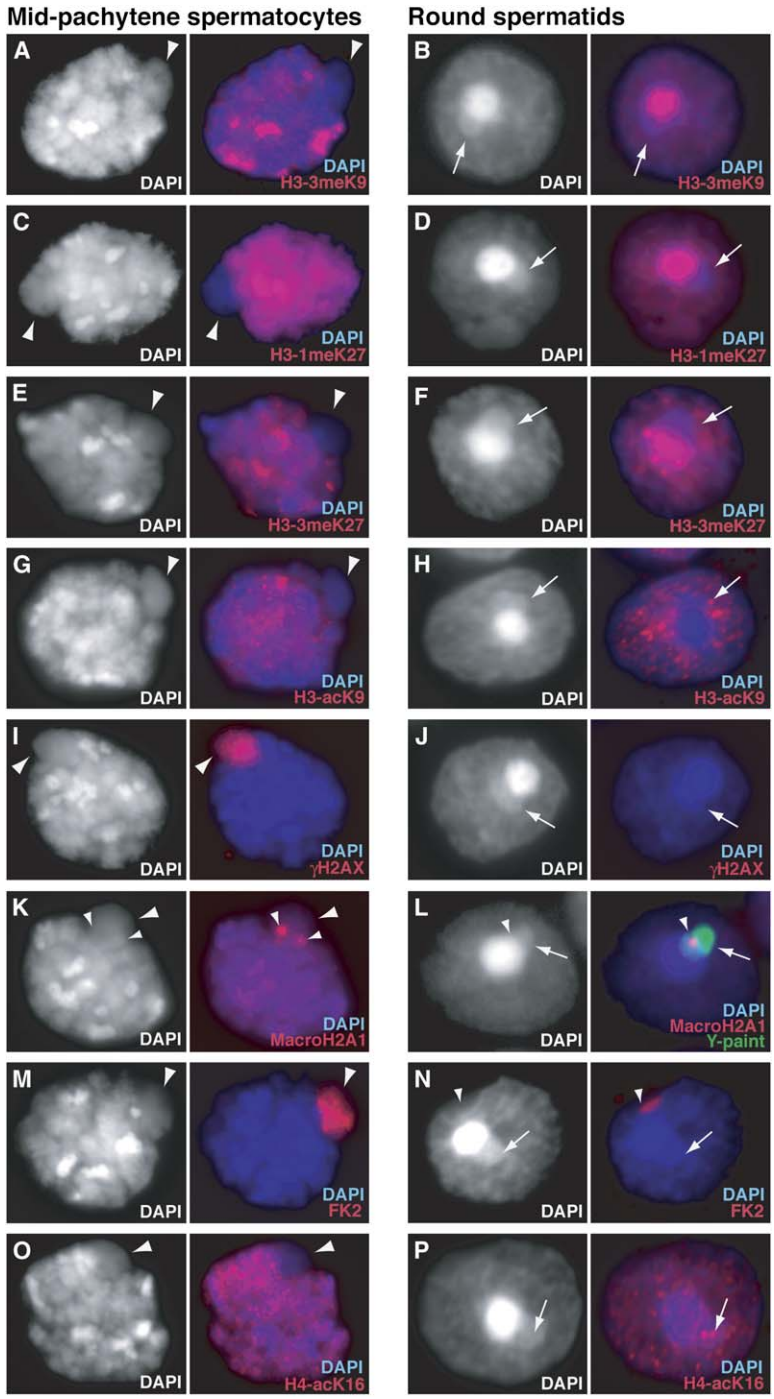

Figure 3. Further Epigenetic Comparison between the XY Body and PMSC

Immunofluorescence detecting various chromatin marks (red signals) as indicated in the cell types noted. All images are single z-sections. Arrowheads, XY body. Arrows, PMSC. Small arrowheads indicate X and Y centromeres in (K), Y centromere in (L), and acrosomal granule in (N).

HP1 is recruited by dimethylation of H3-K9 (H3-2meK9) [17]. Accordingly, late pachytene and diplotene cells displayed robust H3-2meK9 staining on the XY body (80%, n = 26), while this was not the case for mid-pachytene cells (94% with low H3-2meK9, n = 48) (Figures 2K and 2L). In secondary spermatocytes, H3-2meK9 remained enriched on the X and Y (Figures 2M and 2N) [5]. Contrary to previous observation [5], we further found that the H3-2meK9 mark persisted in round spermatids on both X- and Y-PMSC (Figures 2O and 2P; 66% of nuclei, n = 178) (34% showed diffused nuclear staining; Figure S3A).

The dynamics of H3-K9 trimethylation (H3-3meK9) and H3-K27 mono- and trimethylation (H3-1meK27 and H3-3meK27) were also similar between the XY body and PMSC. H3-3meK9 was not enriched on the XY body nor PMSC at any time (Figures 3A and 3B and data not shown). In contrast, H3-1meK27 and H3-3meK27 were specifically excluded from the XY body (Figures 3C and 3E), the segregated X and Y of secondary spermatocytes (data not shown), and PMSC of round spermatids (Figures 3D and 3F; 100% exclusion, n = 53 for H3-1meK27; 100%, n = 64 for H3-3meK27). H3-K9 acetylation patterns were also excluded from the XY body to

PMSC of round spermatids (Figures 3G and 3H). These similarities from XY body to PMSC suggest that meiotic and postmeiotic silencing is a continuous process.

The XY body and PMSC were not identical in every respect, however. First, while histone H2AX was phosphorylated (γH2AX) on the XY body (Figure 3I), γH2AX did not persist beyond diplotene of meiosis I [18] and was not observed on PMSC (Figure 3J). Furthermore, while macroH2A1 associated with the XY body (Figure 3K) [16], it did not localize to X-PMSC in round spermatids (0%, n = 87; data not shown). A small focus of macroH2A1 did remain on the Y centromere of secondary spermatocytes (data not shown) and Y-PMSC in round spermatids (100%, n = 111; Figure 3L) [16]. Additionally, while the XY body and female X_i were ubiquitylated on H2A (Figure 3M and data not shown) [19–21], no PMSC displayed this mark (Figure 3N). Finally, while H4-acK16 was excluded from XY body (Figure 3O), H4-acK16 was diffusely present in round spermatids (Figure 3P). Thus, although the XY body and PMSC appear continuous, the X and Y are progressively remodelled from meiosis to spermiogenesis.

Microarray Analysis of the Male Germline X Chromosome

To examine X chromosome expression on a gene-by-gene basis, we next performed microarray analysis on four spermatic subpopulations, including type A and type B spermatogonia (AS, BS), pachytene spermatocytes (PS), and steps 1–8 round spermatids (RS). On Affymetrix MG-430 2.0 chips, 1306 X-linked loci represented 676 distinct genes. Of these, 379 genes (Groups A–D) were expressed at some time during spermatogenesis, while the remaining 297 genes (Group E) had very low or undetectable expression at any stage (Figure 4A; Table S1).

To obtain a chromosome-specific average, we calculated the mean expression value across all genes on the X, Y, or autosomes (Figure 4B). While the average did not vary significantly on autosomes across the four cell types, the X showed a pachytene-specific downregulation with only a partial recovery in round spermatids (Figure 4B, Figure S4). We used Pearson's χ^2 analysis to test the null hypothesis that levels in PS and RS did not decrease relative to the spermatogonial average, [(AS + BS)/2]. In a two-group comparison between [(AS + BS)/2] versus PS and [(AS + BS)/2] versus RS by a one-sided test, we found the differences to be highly significant on the X, with $p < 10E\text{-}15$ with respect to PS and $p = 3.0 \times 10E\text{-}11$ with respect to RS. In contrast, the same test applied to all autosomal genes gave $p > 0.5$ with respect to both PS and RS.

For the 379 expressed X genes, we created a visual "heatmap" to follow their expression pattern in AS, BS, PS, and RS (Figure 4C). Along the vertical axis, genes were hierarchically clustered based on expression across the four cell types. For each gene, the expression level was represented along a red-to-green color gradient, with red denoting the highest and green denoting the lowest level for a given gene. In cases where the X genes were expressed premeiotically, nearly all were suppressed or significantly downregulated in PS, demonstrating that MSCI globally silences the X and Y. Significantly, a large majority of genes showed continued repression in RS. In contrast, autosomal expression bore no relationship to MSCI. On the Y, only 10 genes (on the chip) were expressed, thereby precluding general conclusions about Y expression patterns. Nonetheless, Y genes appeared to reactivate after MSCI, possibly because spermiogenesis-specific genes, such *Ssty1* and *Ssty2*, were represented in the Y subset (Figure 4B and Table S1). Similar results were obtained with microarray analysis by means of MG-U74v2 chips (data not shown) and RT-PCR of select genes (Figure S5). Real-time RT-PCR values for each gene were normalized to that of β-actin, a gene whose expression did not fluctuate significantly among the four cell types (data not shown). Among 19 genes tested on the X, 14 showed repression in RS, including those with autosomal retrogenes such as *G6pdx*, *Pgk1*, and *Pdha1*. Five of 19 genes displayed activity in RS, including *Ube1x* and *Ube2a*, consistent with previous reports [6, 7].

We next determined the extent to which pachytene-repressed genes "recovered" their expression (Figure 4D). To determine whether a specific gene was repressed in PS, we used the criterion:

$$0.5 \times \max(E_{AS}, E_{BS}) > E_{PS},$$

where E represented expression of the cell type denoted by the subscript. By this criterion, a gene that showed pachytene signal intensity at <50% of that in AS or BS was defined as "repressed." To determine whether a pachytene-repressed gene was reactivated after meiosis, we calculated the "recovery rate" in RS as follows:

$$\text{Recovery rate} = \{E_{RS} - E_{PS}\}/\{\max(E_{AS}, E_{BS}) - E_{PS}\}.$$

On this basis, five groups of X genes were evident (Figures 4A, 4E, and 4F, Table S2). Of 379 active X genes, 311 were expressed in spermatogonia and all were subject to MSCI (Figure 4A). Significantly, the vast majority (278/311) remained silent after meiosis. Group A genes included *Hprt1*, *Mecp2*, and *Pdha1* and showed an average expression in RS that was barely above PS levels (Figure 4D, inset). Only 33 showed a recovery rate of >0.5 in RS (Group B, e.g., *Pctk1, Ube2a*, and *Pdk3*). This indicated that only 10.6% (33/311) of spermatogonially expressed genes reactivated after meiosis. Group C genes were expressed only in RS (e.g., *Arp-T1* [sperm head protein] and *Akap4* [flagellum protein]). Group D genes resembled Group A genes in that they were downregulated in PS and/or repressed in RS, but could not strictly be classified as A because their PS levels slightly exceeded $0.5 \times \max(E_{AS}, E_{BS})$ (possibly due to long transcript half-lives). Finally, Group E were not expressed at any time during spermatogenesis.

Taken together, these data demonstrated that 87.0% of 676 X genes are suppressed in RS (278 Group A + 13 D + 297 E = 588). Notably, this degree of suppression is comparable to that for the inactive human X, on which 75%–85% of genes are suppressed [22]. Thus, postmeiotic X silencing is extensive. In contrast to the zygotic X^P [10], the strength of PMSC silencing did not vary with distance from the X-inactivation center (*Xic*) (Figures 4G and 4H; Table S3), perhaps in keeping with the fact that MSCI [7, 23] and possibly also PMSC silencing do not depend on *Xist*, while imprinted XCI in the embryo requires *Xist* [24]. However, active genes in Groups B

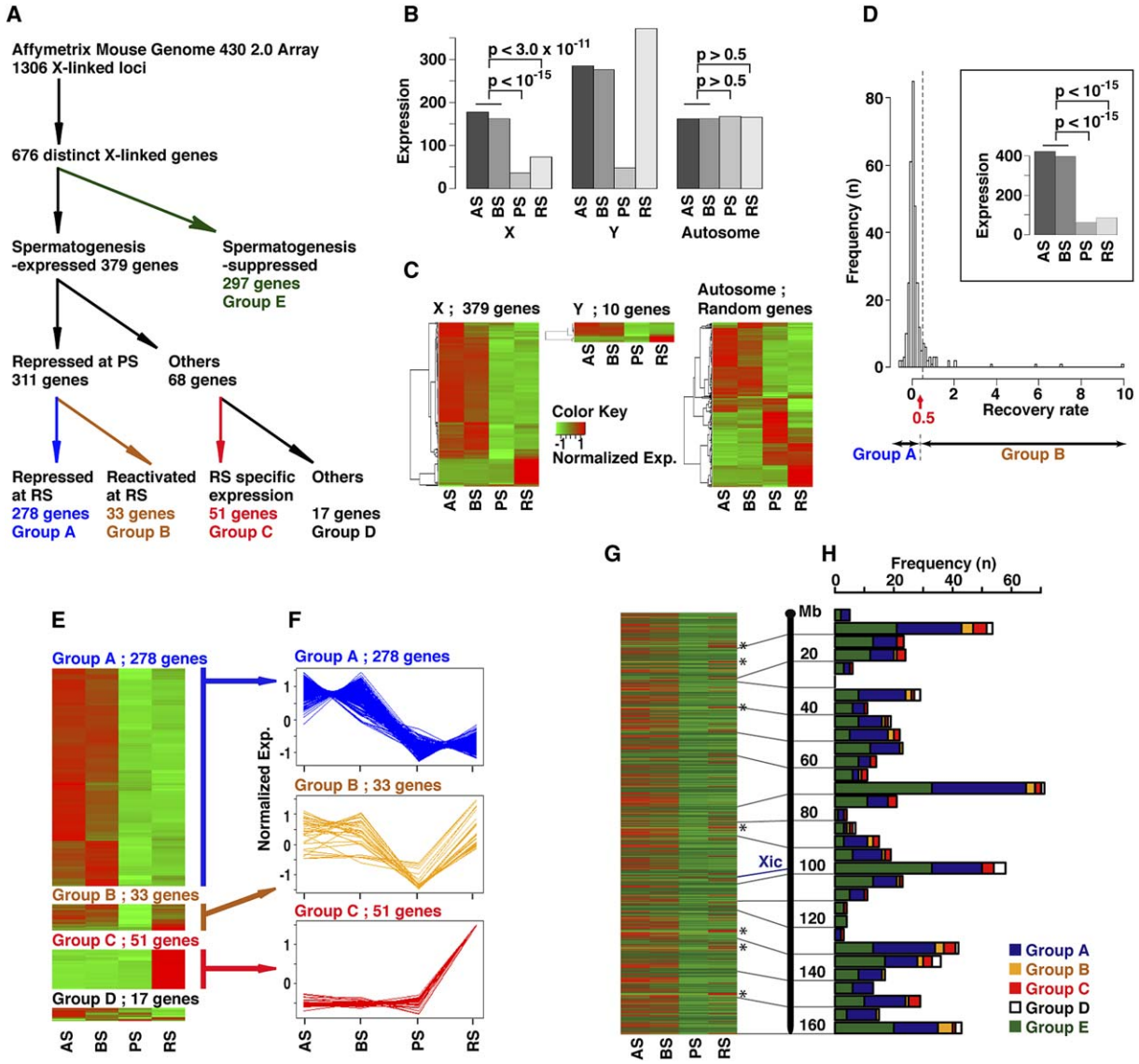

Figure 4. Microarray Analysis of the X in Male Germ Cells

(A) Classification of X genes according to their expression pattern during spermatogenesis.

(B) Mean expression level of all genes on the X, Y, and autosomes. p derived from Pearson's χ^2 analysis.

(C) Expression heatmaps of the X, Y, and autosomal genes. For autosomes, 1000 genes were randomly selected by a computer program.

(D) Histogram of recovery rates from 311 PS-repressed genes. Inset, mean expression levels of the 311 genes.

(E) Heatmaps of normalized gene expression profiles for each gene group.

(F) Developmental profiles of each group shown in (E).

(G) Heatmap of 676 X genes ordered according to their position along the X chromosome. Group E genes are represented on the heatmap by an invariant olive color across all stages.

(H) Frequency of Groups A–E genes binned at 5 Mb intervals. Asterisks denote clusters of Group C genes.

and C tend to cluster (Figure 4G, asterisks), suggesting domain-specific features for escape from PSMC silencing. Thus, while PMSC and the zygotic X^P resembled each other in having incomplete inactivation, they differ in how distance from the *Xic* influences silencing.

Discussion

We have discovered that the postmeiotic X occupies a novel nuclear compartment in the male germline and is transcriptionally suppressed on 87% of its genes. The X-PMSC adopts a non-Rabl configuration (as does Y-PMSC) and persists as a hypoactive structure from meiosis II to the end of spermiogenesis. Because PMSC is already evident in the secondary spermatocyte, we propose that PMSC descends directly from the XY body. Thus, X chromosome silencing initiated by MSCI does not end with the dismantling of the XY body, but is maintained in the secondary spermatocyte and PMSC during spermiogenesis (Figure 5).

Despite the continuity of XY body and PMSC, the X-chromatin is progressively remodelled. First, γ-H2AX, ATR, BRCA1, macroH2A1, and H2A-ubiquitylation appear during the intiation of MSCI (Figure 3) [18–20,

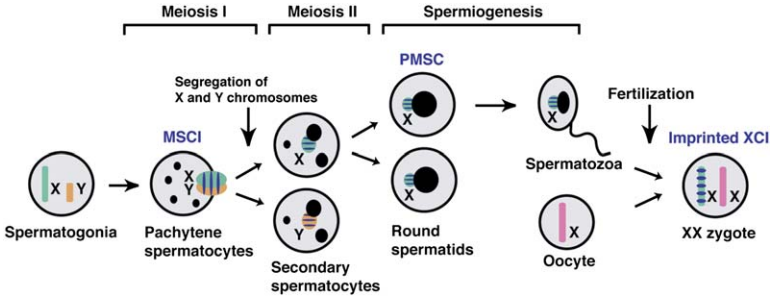

Figure 5. Model: A Continuity of Silencing from XY Body to PMSC to the Imprinted X^P

The silencing initiated by MSCI during meiosis I persists into meiosis II and spermiogenesis (PMSC). The X is then delivered to the zygote as a preinactivated X, accounting for the imprinted X^P of the early mouse embryo. Barred chromosomes represent suppressed transcription. Black circles represent pericentromic heterochromatin or chromocenter.

25, 26]. Once the XY body is established, H3-2meK9, HP1β, and HP1γ accumulate at the pachytene-diplotene transition and persist into PMSC, while γ-H2AX, macroH2A1, and H2A-ubiquitylation are lost (Figures 2 and 3). These late marks may carry through silencing from meiosis to spermiogenesis. Furthermore, because mature spermatozoa retain 2%–15% of histones [27, 28] and associated proteins such as HP1β [29], such marks may provide the basis for inheritance of transcription states (see below).

Our analysis demonstrates that the X is treated differently from autosomes during meiosis and after. What physiologic purpose could this serve? We consider two hypotheses. First, according to theories of sex chromosome evolution, the X accumulates female reproductive genes over time, while the Y accumulates male reproductive genes [30]. If so, one possible raison d'etre of PMSC may be to suppress oogenesis-promoting genes that might interfere with spermiogenesis. A second and not mutually exclusive possibility is that PMSC facilitates dosage compensation by enabling transmission of a partially preinactivated X^P to the embryo [10]. MSCI may be based on MSUD (meiotic silencing by unpaired DNA) [20, 26]—the idea that the sex chromosomes are silenced by virtue of their being incompletely synapsed during pachytene. Indeed, a parallel work suggests that MSUD leads directly to PMSC in the round spermatid [31]. As fathers transmit the X only to daughters, MSUD-driven X^P silencing would have instantly achieved dosage compensation between daughters and sons as the Y degenerated in increments over time [32, 33].

Based on current data, we suggest that preinactivation offers a most parsimonious origin for imprinted X^P-inactivation in the zygote (Figure 5). However, the conclusion is not mutually exclusive with the "de novo inactivation" hypothesis, which proposes that imprinted XCI does not occur until the 4- to 8-cell stage [34]. The continuity of silencing from XY body to zygotic X^P is genetically separable: while MSCI is *Xist* independent, imprinted XCI depends on *Xist* [7, 23, 24]. In *C. elegans*, MSUD-mediated silencing of X^P is lost after ~5 zygotic divisions [35]. Likewise in mammals, the inherited X^P may reactivate without recruiting the secondary *Xist*-dependent silencing mechanism. Thus, a two-step process in which germline silencing requires a de novo *Xist* mechanism to maintain zygotic silencing would reconcile the preinactivation and de novo hypotheses.

Supplemental Data

Supplemental Data include five figures, three tables, and Supplemental Experimental Procedures and can be found with this article online at http://www.current-biology.com/cgi/content/full/16/7/660/DC1/.

Acknowledgments

We thank R. Scully for providing the γH2AX antibody; C. Small and R. Yang for assistance with microarray analysis; J. Atencio for RNA preparation of sperm fractions; K.D. Huynh and all lab members for discussion throughout this work; and M.E. Donohoe, M.C. Anguera, Y. Ogawa, and F.N. Hamada for critical reading of the manuscript. S.H.N. is also grateful to K. Sakaguchi for support during the postdoc transition and is a research fellow of Japan Society for Promotion of Science. J.T.L. is an Investigator of the Howard Hughes Medical Institute. This work was supported by NIH grants GM58839 to J.T.L., GM67825 to P.J.P., HD10808 to M.D.G., and HD46637 to J.R.M.

Received: January 25, 2006
Accepted: January 27, 2006
Published: April 3, 2006

References

1. McKee, B.D., and Handel, M.A. (1993). Sex chromosomes, recombination, and chromatin conformation. Chromosoma *102*, 71–80.
2. Baarends, W.M., and Grootegoed, J.A. (2003). Chromatin dynamics in the male meiotic prophase. Cytogenet. Genome Res. *103*, 225–234.
3. Hoyer-Fender, S. (2003). Molecular aspects of XY body formation. Cytogenet. Genome Res. *103*, 245–255.
4. Handel, M.A. (2004). The XY body: a specialized meiotic chromatin domain. Exp. Cell Res. *296*, 57–63.
5. Khalil, A.M., Boyar, F.Z., and Driscoll, D.J. (2004). Dynamic histone modifications mark sex chromosome inactivation and reactivation during mammalian spermatogenesis. Proc. Natl. Acad. Sci. USA *101*, 16583–16587.
6. Hendriksen, P.J., Hoogerbrugge, J.W., Themmen, A.P., Koken, M.H., Hoeijmakers, J.H., Oostra, B.A., van der Lende, T., and Grootegoed, J.A. (1995). Postmeiotic transcription of X and Y chromosomal genes during spermatogenesis in the mouse. Dev. Biol. *170*, 730–733.
7. McCarrey, J.R., Watson, C., Atencio, J., Ostermeier, G.C., Marahrens, Y., Jaenisch, R., and Krawetz, S.A. (2002). X-chromosome inactivation during spermatogenesis is regulated by an Xist/Tsix-independent mechanism in the mouse. Genesis *34*, 257–266.
8. Wang, P.J., McCarrey, J.R., Yang, F., and Page, D.C. (2001). An abundance of X-linked genes expressed in spermatogenesis. Nat. Genet. *27*, 422–426.
9. Huynh, K.D., and Lee, J.T. (2001). Imprinted X inactivation in eutherians: a model of gametic execution and zygotic relaxation. Curr. Opin. Cell Biol. *13*, 690–697.
10. Huynh, K.D., and Lee, J.T. (2003). Inheritance of a pre-inactivated paternal X chromosome in early mouse embryos. Nature *426*, 857–862.
11. Lyon, M.F. (1999). Imprinting and X chromosome inactivation. In Results and Problems in Cell Differentiation, R. Ohlsson, ed. (Heidelberg: Springer-Verlag), pp. 73–90.

12. McCarrey, J.R. (2001). X-chromosome inactivation during spermatogenesis: the original dosage compensation mechanism in mammals? In Gene Families: Studies of DNA, RNA, Enzymes, and Proteins, G. Xue, Y. Xue, Z. Xu, R. Holmes, G. Hammond, and H.A. Lim, eds. (New Jersey: World Scientific Publishing Company), pp. 59–72.
13. Russell, R.D., Ettlin, R.A., ShinhaHikim, A.P., and Clegg, E.D. (1990). Histological and Histopathological Evaluation of the Testis (Clearwater, FL: Cache River Press).
14. Hall, L.L., Byron, M., Sakai, K., Carrel, L., Willard, H.F., and Lawrence, J.B. (2002). An ectopic human XIST gene can induce chromosome inactivation in postdifferentiation human HT-1080 cells. Proc. Natl. Acad. Sci. USA *99*, 8677–8682.
15. Leitch, A.R. (2000). Higher levels of organization in the interphase nucleus of cycling and differentiated cells. Microbiol. Mol. Biol. Rev. *64*, 138–152.
16. Turner, J.M., Burgoyne, P.S., and Singh, P.B. (2001). M31 and macroH2A1.2 colocalise at the pseudoautosomal region during mouse meiosis. J. Cell Sci. *114*, 3367–3375.
17. Lachner, M., O'Carroll, D., Rea, S., Mechtler, K., and Jenuwein, T. (2001). Methylation of histone H3 lysine 9 creates a binding site for HP1 proteins. Nature *410*, 116–120.
18. Mahadevaiah, S.K., Turner, J.M., Baudat, F., Rogakou, E.P., de Boer, P., Blanco-Rodriguez, J., Jasin, M., Keeney, S., Bonner, W.M., and Burgoyne, P.S. (2001). Recombinational DNA double-strand breaks in mice precede synapsis. Nat. Genet. *27*, 271–276.
19. Baarends, W.M., Hoogerbrugge, J.W., Roest, H.P., Ooms, M., Vreeburg, J., Hoeijmakers, J.H., and Grootegoed, J.A. (1999). Histone ubiquitination and chromatin remodeling in mouse spermatogenesis. Dev. Biol. *207*, 322–333.
20. Baarends, W.M., Wassenaar, E., van der Laan, R., Hoogerbrugge, J., Sleddens-Linkels, E., Hoeijmakers, J.H., de Boer, P., and Grootegoed, J.A. (2005). Silencing of unpaired chromatin and histone H2A ubiquitination in mammalian meiosis. Mol. Cell. Biol. *25*, 1041–1053.
21. de Napoles, M., Mermoud, J.E., Wakao, R., Tang, Y.A., Endoh, M., Appanah, R., Nesterova, T.B., Silva, J., Otte, A.P., Vidal, M., et al. (2004). Polycomb group proteins Ring1A/B link ubiquitylation of histone H2A to heritable gene silencing and X inactivation. Dev. Cell *7*, 663–676.
22. Carrel, L., and Willard, H.F. (2005). X-inactivation profile reveals extensive variability in X-linked gene expression in females. Nature *434*, 400–404.
23. Turner, J.M., Mahadevaiah, S.K., Elliott, D.J., Garchon, H.J., Pehrson, J.R., Jaenisch, R., and Burgoyne, P.S. (2002). Meiotic sex chromosome inactivation in male mice with targeted disruptions of Xist. J. Cell Sci. *115*, 4097–4105.
24. Marahrens, Y., Panning, B., Dausman, J., Strauss, W., and Jaenisch, R. (1997). Xist-deficient mice are defective in dosage compensation but not spermatogenesis. Genes Dev. *11*, 156–166.
25. Turner, J.M., Aprelikova, O., Xu, X., Wang, R., Kim, S., Chandramouli, G.V., Barrett, J.C., Burgoyne, P.S., and Deng, C.X. (2004). BRCA1, histone H2AX phosphorylation, and male meiotic sex chromosome inactivation. Curr. Biol. *14*, 2135–2142.
26. Turner, J.M., Mahadevaiah, S.K., Fernandez-Capetillo, O., Nussenzweig, A., Xu, X., Deng, C.X., and Burgoyne, P.S. (2005). Silencing of unsynapsed meiotic chromosomes in the mouse. Nat. Genet. *37*, 41–47.
27. Gatewood, J.M., Cook, R.G., Balhorn, R., Bradbury, E.M., and Schmid, C.W. (1987). Sequence-specific packaging of DNA in human sperm chromatin. Science *236*, 962–964.
28. Bench, G.S., Friz, A.M., Corzett, M.H., Morse, D.H., and Balhorn, R. (1996). DNA and total protamine masses in individual sperm from fertile mammalian subjects. Cytometry *23*, 263–271.
29. Hoyer-Fender, S., Singh, P.B., and Motzkus, D. (2000). The murine heterochromatin protein M31 is associated with the chromocenter in round spermatids and is a component of mature spermatozoa. Exp. Cell Res. *254*, 72–79.
30. Charlesworth, B. (1991). The evolution of sex chromosomes. Science *251*, 1030–1033.
31. Turner, J.M., Mahadevaiah, S.K., Ellis, P.J., Mitchell, M.J., and Burgoyne, P.S. (2006). Pachytene asynapsis drives meiotic sex chromosome inactivation and leads to substantial post-meiotic repression in spermatids. Dev. Cell *10*, in press.
32. Lee, J.T. (2003). Molecular links between X-inactivation and autosomal imprinting: X-inactivation as a driving force for the evolution of imprinting. Curr. Biol. *13*, R242–R254.
33. Huynh, K.D., and Lee, J.T. (2005). Opinion: X-chromosome inactivation: a hypothesis linking ontogeny and phylogeny. Nat. Rev. Genet. *6*, 410–418.
34. Okamoto, I., Otte, A.P., Allis, C.D., Reinberg, D., and Heard, E. (2004). Epigenetic dynamics of imprinted X inactivation during early mouse development. Science *303*, 644–649.
35. Bean, C.J., Schaner, C.E., and Kelly, W.G. (2004). Meiotic pairing and imprinted X chromatin assembly in *Caenorhabditis elegans*. Nat. Genet. *36*, 100–105.

Accession Numbers

The microarray data for Figures 4 and S4 and Tables S1, S2, and S3 have been uploaded to the GEO database (http://www.ncbi.nlm.nih.gov/geo) with the accession number GSE4193.